2012

The Development of High-Resolution Seafloor Mapping Techniques

Chris Roman
University of Rhode Island, croman2@uri.edu

Gabrielle Inglis
University of Rhode Island, gabrielle.inglis@gmail.com

See next page for additional authors

Citation/Publisher Attribution

Roman, C., Inglis, G., Vaughn, J. I., Smart, C., Douillard, B., & Williams, S. (2012). The development of high-resolution seafloor mapping techniques. In K. L. C. Bell, K. Elliot, C. Martinez, and S. A. Fuller (eds.), New Frontiers in Ocean Exploration: The E/V *Nautilus* and NOAA Ship *Okeanos Explorer* 2011 Field Season. *Oceanography* 25(1), supplement, pp. 42-45.
doi: 10.5670/oceanog.2011.supplement.01

Oceanography
VOL. 25, NO. 1, SUPPLEMENT | MARCH 2012

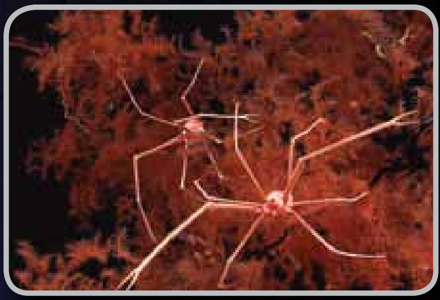

New Frontiers in Ocean Exploration

The E/V *Nautilus* and NOAA Ship *Okeanos Explorer* 2011 Field Season

GUEST EDITORS | KATHERINE L.C. BELL, KELLEY ELLIOTT, CATALINA MARTINEZ, AND SARAH A. FULLER

The Development of High-Resolution Seafloor Mapping Techniques

By Chris Roman, Gabrielle Inglis, J. Ian Vaughn, Clara Smart, Bertrand Douillard, and Stefan Williams

The 2011 field season continued the development of centimeter-level mapping techniques for marine geology, biology, and archaeology. The ROV *Hercules* is equipped with a suite of mapping instruments that enable detailed visual and acoustic seafloor surveys. The mapping sensors include a 1,375 kHz BlueView Technologies multibeam, verged color and black and white 12-bit 1360 × 1024 Prosilica stereo cameras, and a 100 mW 532 nm green laser sheet. The sensors are mounted near the rear of vehicle and arranged to image a common area. The vehicle navigation data comes from an RDI Doppler velocity log (DVL), IXSEA OCTANS fiber-optic gyroscope, and a Paroscientific depth sensor.

During the 2011 field season, one or more of the above sensors mapped 21 shipwrecks (see page 27, Figure 4). At many wrecks in the Black Sea, exceptionally turbid water prevented complete photographic surveys. However, the BlueView sonar worked in all cases and provided bathymetric data with multicentimeter-level resolution. We also continued the use of structured light laser imaging (Roman et al., 2010a) to obtain fine-scale, centimeter-level bathymetric maps of complete shipwrecks (Figure 1). This technique uses a camera to image a laser line projected on the seafloor. If the geometry between the laser and camera is known through calibration, a three-dimensional profile of the bottom can be measured to subcentimeter precision along the laser line. The laser system can produce bathymetry in turbid conditions where standard camera images become too contrast-limited for stereo vision techniques.

The laser system is set up by first calibrating the stereo cameras and then solving for the relationship between the image points on the laser line in the three-dimensional camera frame coordinate system. This year, we developed an in situ calibration procedure that can be used over

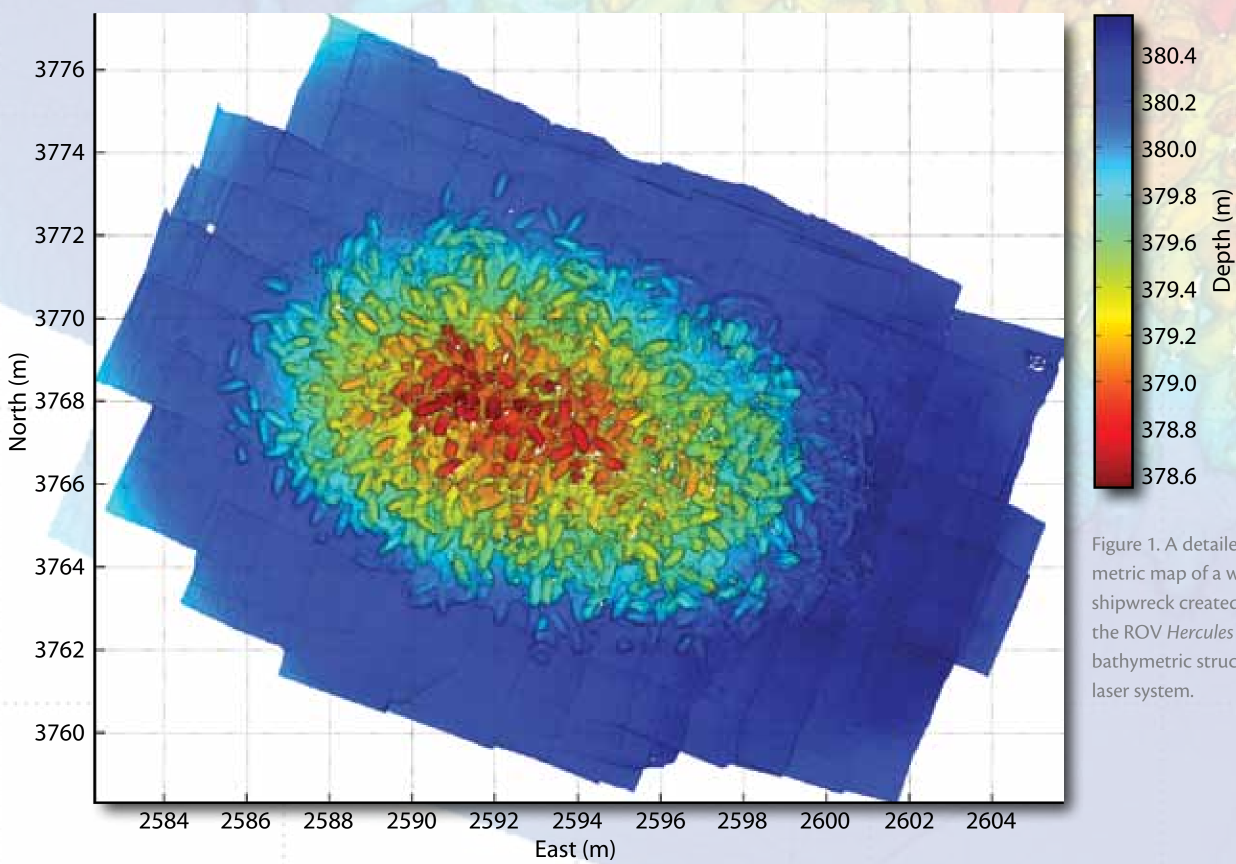

Figure 1. A detailed bathymetric map of a whole shipwreck created with the ROV *Hercules* and the bathymetric structured light laser system.

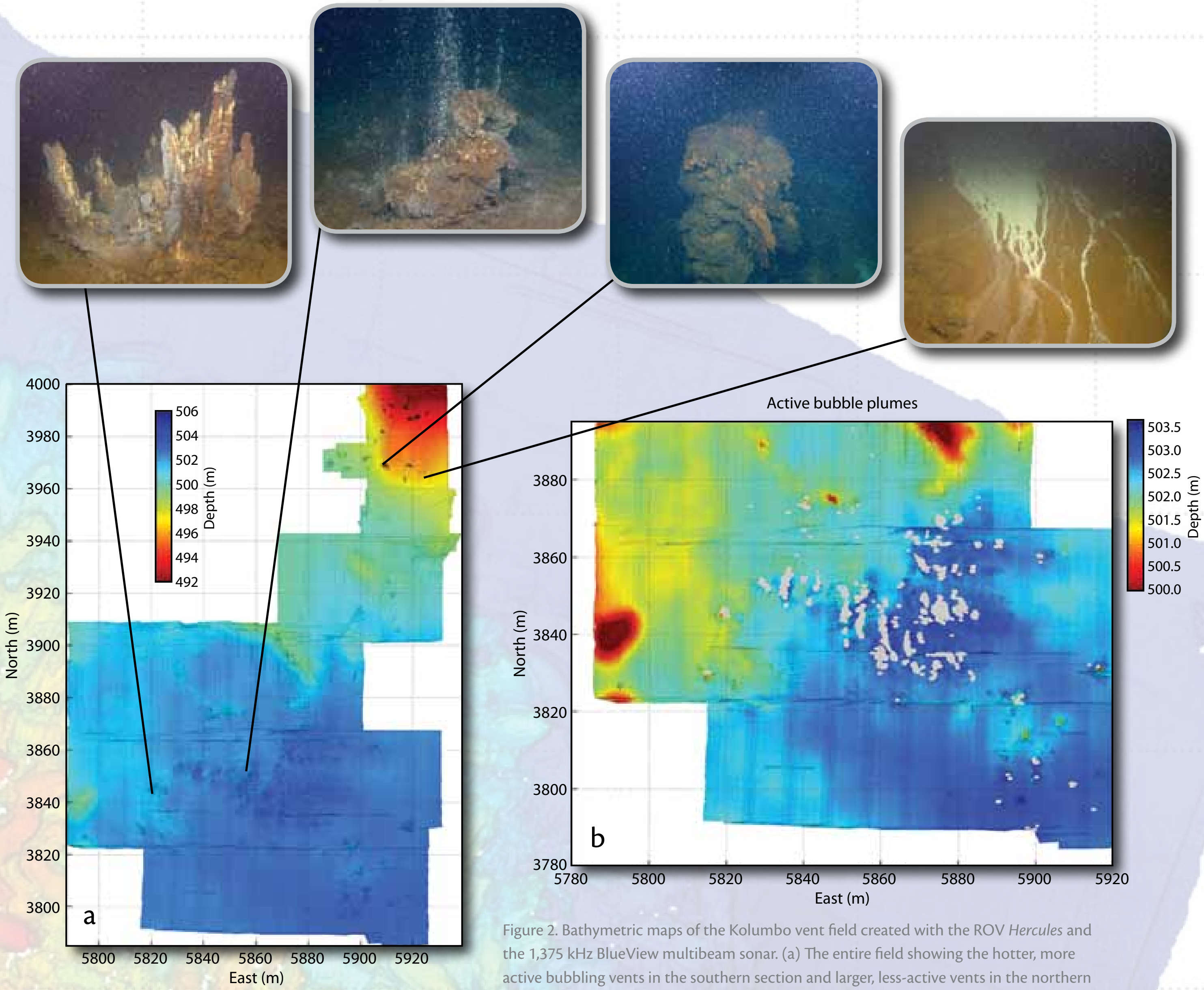

Figure 2. Bathymetric maps of the Kolumbo vent field created with the ROV *Hercules* and the 1,375 kHz BlueView multibeam sonar. (a) The entire field showing the hotter, more active bubbling vents in the southern section and larger, less-active vents in the northern section. (b) A close up of the southern section showing the distribution of active bubble plumes (gray patches) detected by the BlueView sonar (Figure 3).

natural terrain during operations. The approach uses paired feature points automatically extracted from stereo images of the laser line, and the stereo projection places these points in the three-dimensional camera frame. The drawback of this method is that it relies on the accuracy of the stereo calibration, which may be completed in a tank or using additional in situ methods.

To survey complete shipwrecks, we use a previously developed bathymetric simultaneous localization and mapping (SLAM) technique (Roman and Singh, 2007). This method relies on matching sections of the laser data across overlapping tracklines to help reduce the negative effects of position drift in the ROV's dead-reckoned navigation. Our goal is to produce such surveys of areas on the order of tens of meters per side, and at grid resolutions of 5 mm. The ability to make reliable across-track matches in an automated fashion over such complex scenes can be challenging and is a topic of ongoing research.

During exploration of the Hellenic Volcanic Arc, the BlueView sonar was used to create a large bathymetric map covering the known extent of the Kolumbo vent field. This survey was completed at an altitude of 9 m with a trackline spacing of 5 m. The narrow spacing ensured that a full volume at least 5 m above the seafloor was completely resolved. The data were then processed to both resolve the seafloor bathymetry (Figure 2a) and identify the active bubble plumes (Figure 2b). This survey altitude also reduced the navigation problems associated with corruption of the DVL velocity measurements by the bubble plumes.

To identify active plumes, the bubbles were segmented

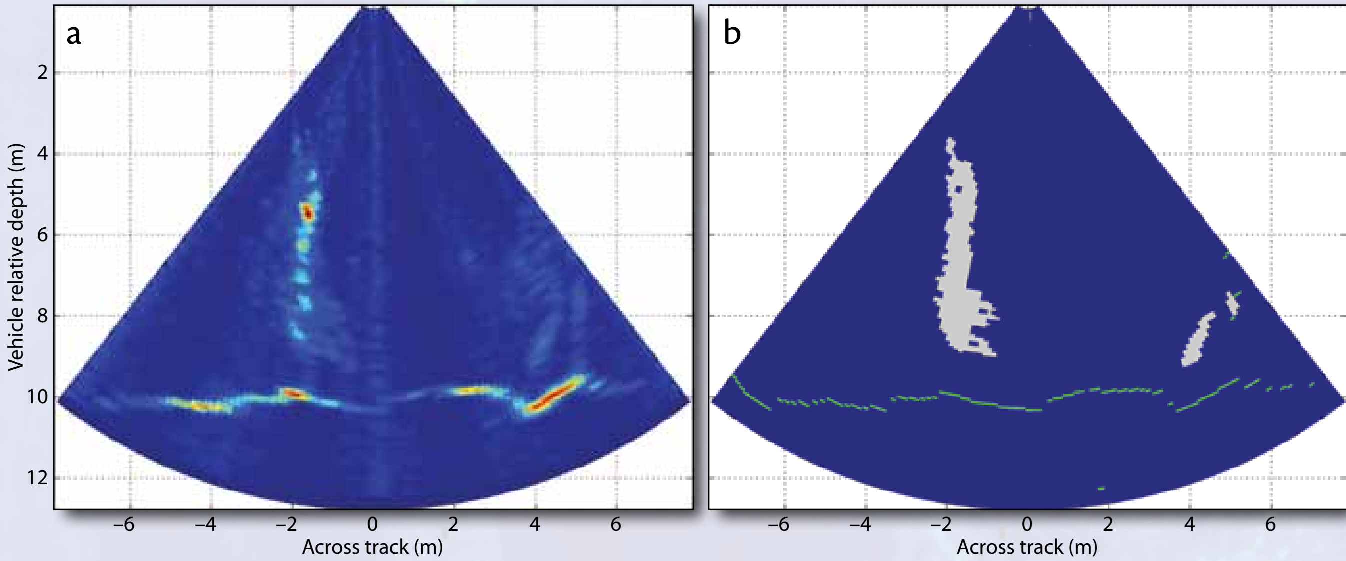

Figure 3. (a) A sample sonar image showing a large bubble plume rising approximately 6 m from the seafloor (left of center) and the edge of a smaller plume (right side). (b) The same ping processed to show the identified bottom (green) and bubbles isolated from water column (gray).

Figure 4. BELOW | Comparison between the 2010 (left) and 2011 (right) photomosaics of the northern vent field area. Differences in the bacterial mat coverage are highlighted. RIGHT | A high-resolution bathymetric map of the mosaic area created with the BlueView sonar during the 2.7 m altitude photomosaic surveys.

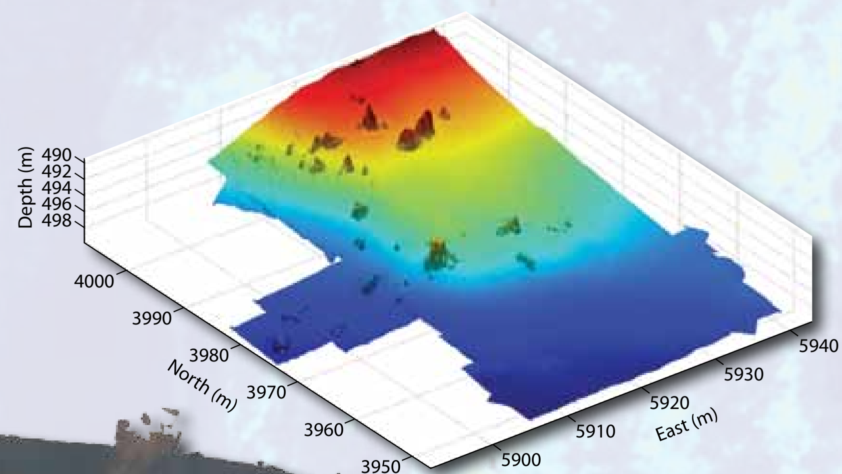

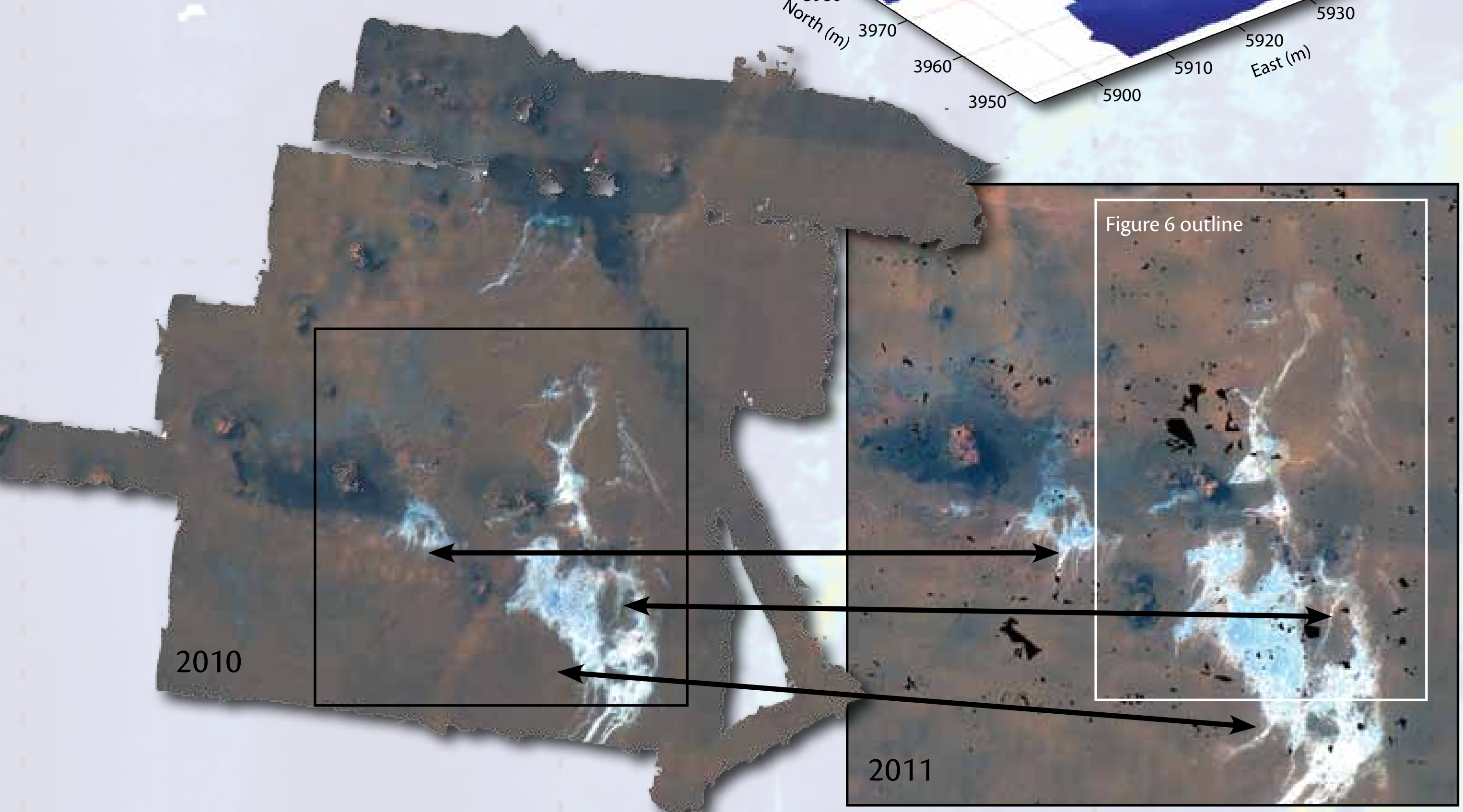

from the water column data (Figure 3a). The algorithm first looked for the bottom by searching back from the maximum range. Once detected, the bottom was then excluded from the sonar image so the bubbles could be identified by isolating the water column values above a multiple of the mean background signal level. The pixels identified as bubbles were then cleaned using several morphological filtering operations to consolidate the identified plumes and remove spurious points (Figure 3b). Passes over the most active areas of the field showed the largest bubble plumes extending approximately 12 m from the seafloor before being dissolved. The bubble plumes were found emanating from a subset of chimney features as well as some relatively flat areas of the seafloor (Figure 2a).

At the northern end of the vent field, a comparison between photomosaics completed in 2010 and 2011 shows a change in the bacterial mat covering the seafloor (Figure 4; Mahon et al., 2008; Johnson-Roberson et al., 2010). Some differences in the overall shape and several new streams of bacteria are evident. These surveys were completed at a 2.7 m altitude due to the persistent turbidity in the area (Figure 2).

A smaller bathymetric survey centered on the bacterial mat area was also completed using the green laser. This survey was used to map the fine-scale bathymetry of what seemed to be downhill flow channels and to locate areas of diffuse water venting over the bacterial mat. The presence of venting fluid can be detected by looking at the quality of the imaged laser line. The laser will refract as it passes through the warm water and appear blurred in the image (Figure 5). By batch processing the laser data and computing pixel intensity moments in the vertical image dimension about the center of the laser line, the amount of blur can be quantified and color-coded as a proxy for venting intensity (Figure 6). The basic spatial pattern of the bacterial map seen in the photomosaic (Figure 4) can also be seen here. Visual inspection confirmed varying amounts of shimmering water over the extent of the mat. Temperature probes taken with *Hercules* indicate vent temperatures between 30° and 60°C above ambient in the area.

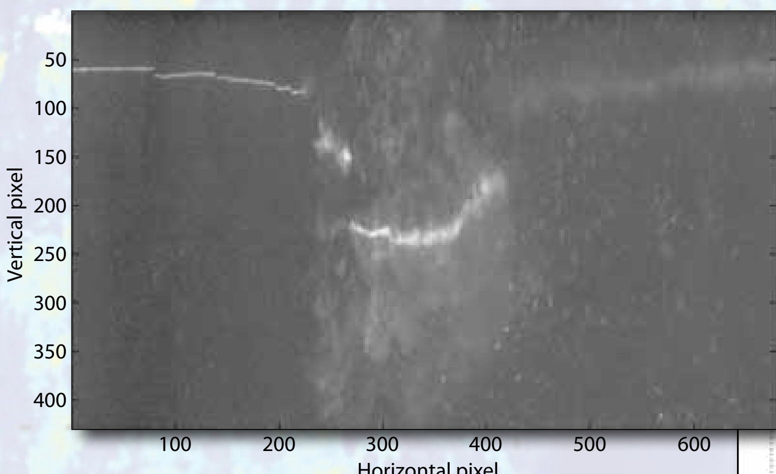

Figure 5. A 2 m wide sample image showing the laser line projected on the seafloor. The crisp line (left side) is undisturbed, while refraction due to hot water venting (center and right side) blurs the line.

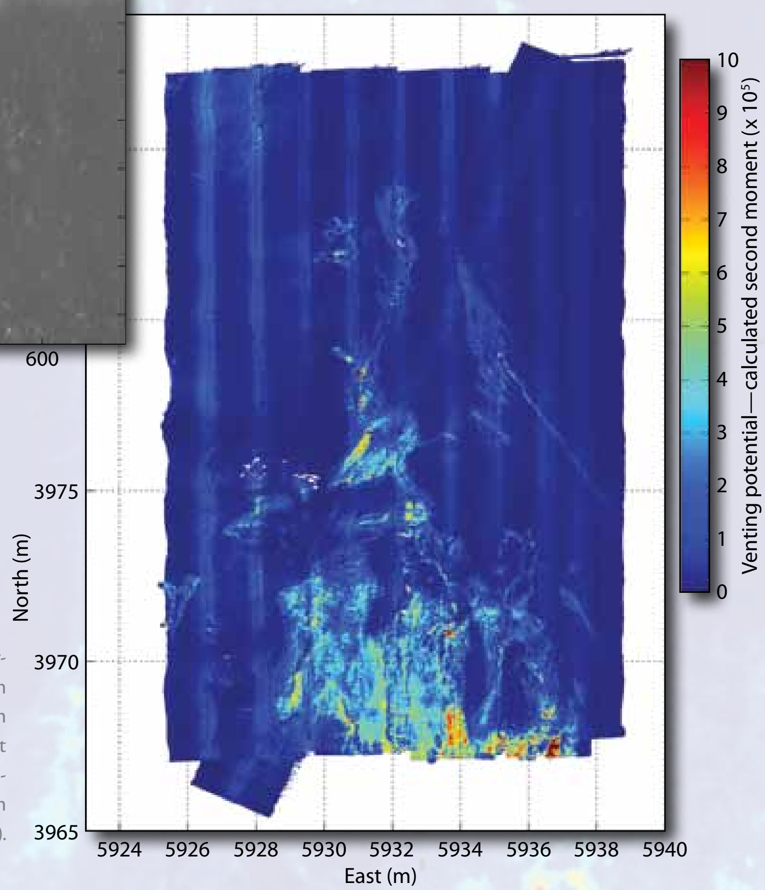

Figure 6. A seafloor map color-coded to show the distribution and intensity of active venting in the vicinity of the bacterial mat (Figure 4). The color scale indicates the degree of blurring seen in the laser line (Figure 5).